Eur. Phys. J. C 26, 527–538 (2003)
Digital Object Identifier (DOI) 10.1140/epjc/s2002-01118-x

THE EUROPEAN PHYSICAL JOURNAL C

The Q^2–dependence of the generalised Gerasimov–Drell–Hearn integral for the deuteron, proton and neutron

The HERMES Collaboration

A. Airapetian[32], N. Akopov[32], Z. Akopov[32], M. Amarian[26,32], V.V. Ammosov[24], E.C. Aschenauer[6], R. Avakian[32], A. Avetissian[32], E. Avetissian[10,32], P. Bailey[15], V. Baturin[23], C. Baumgarten[21], M. Beckmann[5], S. Belostotski[23], S. Bernreuther[29], N. Bianchi[10], H.P. Blok[22,30], H. Böttcher[6], A. Borissov[19], O. Bouhali[22], M. Bouwhuis[15], J. Brack[4], S. Brauksiepe[11], A. Brüll[18], I. Brunn[8], G.P. Capitani[10], H.C. Chiang[15], G. Ciullo[9], G.R. Court[16], P.F. Dalpiaz[9], R. De Leo[3], L. De Nardo[1], E. De Sanctis[10], E. Devitsin[20], P. Di Nezza[10], M. Düren[13], M. Ehrenfried[6], A. Elalaoui-Moulay[2], G. Elbakian[32], F. Ellinghaus[6], U. Elschenbroich[11], J. Ely[4], R. Fabbri[9], A. Fantoni[10], A. Fechtchenko[7], L. Felawka[28], H. Fischer[11], B. Fox[4], J. Franz[11], S. Frullani[26], Y. Gärber[8], G. Gapienko[24], V. Gapienko[24], F. Garibaldi[26], E. Garutti[22], G. Gavrilov[23], V. Gharibyan[32], G. Graw[21], O. Grebeniouk[23], P.W. Green[1,28], L.G. Greeniaus[1,28], A. Gute[8], W. Haeberli[17], K. Hafidi[2], M. Hartig[28], D. Hasch[10], D. Heesbeen[22], F.H. Heinsius[11], M. Henoch[8], R. Hertenberger[21], W.H.A. Hesselink[22,30], A. Hillenbrand[8], Y. Holler[5], B. Hommez[12], G. Iarygin[7], A. Izotov[23], H.E. Jackson[2], A. Jgoun[23], R. Kaiser[14], E. Kinney[4], A. Kisselev[23], P. Kitching[1], K. Königsmann[11], H. Kolster[18], M. Kopytin[23], V. Korotkov[6], E. Kotik[1], V. Kozlov[20], B. Krauss[8], V.G. Krivokhijine[7], L. Lagamba[3], L. Lapikás[22], A. Laziev[22,30], P. Lenisa[9], P. Liebing[6], T. Lindemann[5], K. Lipka[6], W. Lorenzon[19], N.C.R. Makins[15], H. Marukyan[32], F. Masoli[9], F. Menden[11], V. Mexner[22], N. Meyners[5], O. Mikloukho[23], C.A. Miller[1,28], Y. Miyachi[29], V. Muccifora[10], A. Nagaitsev[7], E. Nappi[3], Y. Naryshkin[23], A. Nass[8], W.-D. Nowak[6], K. Oganessyan[5,10], H. Ohsuga[29], G. Orlandi[26], S. Podiatchev[8], S. Potashov[20], D.H. Potterveld[2], M. Raithel[8], D. Reggiani[9], P.E. Reimer[2], A. Reischl[22], A.R. Reolon[10], K. Rith[8], G. Rosner[14], A. Rostomyan[32], D. Ryckbosch[12], I. Sanjiev[2,23], F. Sato[29], I. Savin[7], C. Scarlett[19], A. Schäfer[25], C. Schill[11], G. Schnell[6], K.P. Schüler[5], A. Schwind[6], J. Seibert[11], B. Seitz[1], R. Shanidze[8], T.-A. Shibata[29], V. Shutov[7], M.C. Simani[22,30], K. Sinram[5], M. Stancari[9], M. Statera[9], E. Steffens[8], J.J.M. Steijger[22], J. Stewart[6], U. Stösslein[4], K. Suetsugu[29], H. Tanaka[29], S. Taroian[32], A. Terkulov[20], O. Teryaev[25], S. Tessarin[9], E. Thomas[10], A. Tkabladze[6], M. Tytgat[12], G.M. Urciuoli[26], P. van der Nat[22,30], G. van der Steenhoven[22], R. van de Vyver[12], M.C. Vetterli[27,28], V. Vikhrov[23], M.G. Vincter[1], J. Visser[22], M. Vogt[8], J. Volmer[6], C. Weiskopf[8], J. Wendland[27,28], J. Wilbert[8], T. Wise[17], S. Yen[28], S. Yoneyama[29], B. Zihlmann[22,30], H. Zohrabian[32], P. Zupranski[31]

[1] Department of Physics, University of Alberta, Edmonton, Alberta T6G 2J1, Canada
[2] Physics Division, Argonne National Laboratory, Argonne, Illinois 60439-4843, USA
[3] Istituto Nazionale di Fisica Nucleare, Sezione di Bari, 70124 Bari, Italy
[4] Nuclear Physics Laboratory, University of Colorado, Boulder, Colorado 80309-0446, USA
[5] DESY, Deutsches Elektronen-Synchrotron, 22603 Hamburg, Germany
[6] DESY Zeuthen, 15738 Zeuthen, Germany
[7] Joint Institute for Nuclear Research, 141980 Dubna, Russia
[8] Physikalisches Institut, Universität Erlangen-Nürnberg, 91058 Erlangen, Germany
[9] Istituto Nazionale di Fisica Nucleare, Sezione di Ferrara and Dipartimento di Fisica, Università di Ferrara, 44100 Ferrara, Italy
[10] Istituto Nazionale di Fisica Nucleare, Laboratori Nazionali di Frascati, 00044 Frascati, Italy
[11] Fakultät für Physik, Universität Freiburg, 79104 Freiburg, Germany
[12] Department of Subatomic and Radiation Physics, University of Gent, 9000 Gent, Belgium
[13] Physikalisches Institut, Universität Gießen, 35392 Gießen, Germany
[14] Department of Physics and Astronomy, University of Glasgow, Glasgow G128 QQ, UK
[15] Department of Physics, University of Illinois, Urbana, Illinois 61801, USA
[16] Physics Department, University of Liverpool, Liverpool L69 7ZE, UK
[17] Department of Physics, University of Wisconsin-Madison, Madison, Wisconsin 53706, USA
[18] Laboratory for Nuclear Science, Massachusetts Institute of Technology, Cambridge, Massachusetts 02139, USA
[19] Randall Laboratory of Physics, University of Michigan, Ann Arbor, Michigan 48109-1120, USA
[20] Lebedev Physical Institute, 117924 Moscow, Russia
[21] Sektion Physik, Universität München, 85748 Garching, Germany
[22] Nationaal Instituut voor Kernfysica en Hoge-Energiefysica (NIKHEF), 1009 DB Amsterdam, The Netherlands
[23] Petersburg Nuclear Physics Institute, St. Petersburg, Gatchina, 188350 Russia
[24] Institute for High Energy Physics, Protvino, Moscow oblast, 142284 Russia

[25] Institut für Theoretische Physik, Universität Regensburg, 93040 Regensburg, Germany
[26] Istituto Nazionale di Fisica Nucleare, Sezione Roma 1, Gruppo Sanità and Physics Laboratory, Istituto Superiore di Sanità, 00161 Roma, Italy
[27] Department of Physics, Simon Fraser University, Burnaby, British Columbia V5A 1S6, Canada
[28] TRIUMF, Vancouver, British Columbia V6T 2A3, Canada
[29] Department of Physics, Tokyo Institute of Technology, Tokyo 152, Japan
[30] Department of Physics and Astronomy, Vrije Universiteit, 1081 HV Amsterdam, The Netherlands
[31] Andrzej Soltan Institute for Nuclear Studies, 00-689 Warsaw, Poland
[32] Yerevan Physics Institute, 375036 Yerevan, Armenia

Received: 20 October 2002 /
Published online: 15 January 2003 –

Abstract. The Gerasimov–Drell–Hearn (GDH) sum rule connects the anomalous contribution to the magnetic moment of the target nucleus with an energy–weighted integral of the difference of the helicity–dependent photoabsorption cross sections. Originally conceived for real photons, the GDH integral can be generalised to the case of photons with virtuality Q^2. For spin–1/2 targets such as the nucleon, it then represents the non-perturbative limit of the first moment Γ_1 of the spin structure function $g_1(x, Q^2)$ in deep inelastic scattering (DIS). The data collected by HERMES with a deuterium target are presented together with a re-analysis of previous measurements on the proton. This provides an unprecedented and complete measurement of the generalised GDH integral for photon–virtuality ranging over $1.2 < Q^2 < 12.0$ GeV^2 and for photon–nucleon invariant mass squared W^2 ranging over $1 < W^2 < 45$ GeV^2, thus covering simultaneously the nucleon-resonance and the deep inelastic scattering regions. These data allow the study of the Q^2–dependence of the full GDH integral, which is sensitive to both the Q^2–evolution of the resonance form factors and contributions of higher twist. The contribution of the nucleon-resonance region is seen to decrease rapidly with increasing Q^2. The DIS contribution is sizeable over the full measured range, even down to the lowest measured Q^2. As expected, at higher Q^2 the data are found to be in agreement with previous measurements of the first moment of g_1. From data on the deuteron and proton, the GDH integral for the neutron has been derived and the proton–neutron difference evaluated. This difference is found to satisfy the fundamental Bjorken sum rule at $Q^2 = 5$ GeV^2.

1 Introduction

The Gerasimov–Drell–Hearn (GDH) sum rule connects an energy–weighted integral of the difference of the helicity–dependent real–photon absorption cross sections with the anomalous contribution $\kappa = \frac{\mu M_t}{eI} - Z$ to the magnetic moment μ of the target nucleus with atomic number Z [1] (or nucleon [1,2]):

$$\int_{\nu_0}^{\infty} \left[\sigma^{\rightrightarrows}(\nu) - \sigma^{\rightleftarrows}(\nu)\right] \frac{d\nu}{\nu} = -\frac{4\pi^2 I\alpha}{M_t^2}\kappa^2. \qquad (1)$$

Here $\sigma^{\rightrightarrows}$ and $\sigma^{\rightleftarrows}$ are the photoabsorption cross sections for relative orientation of the photon spin anti–parallel and parallel to the nucleus spin I, ν is the photon energy in the target rest frame, ν_0 is the photoabsorption threshold, M_t is the nucleus mass, α the electromagnetic fine–structure constant and e the elementary charge. This sum rule provides an interesting link between the helicity–dependent dynamics and a static ground state property of the target nucleus.

The GDH sum rule holds for any type of target, i.e. it is valid for protons, neutrons or nuclei. It is also considered to be important in electroweak physics [3]. The GDH sum rule is derived starting from the Compton forward–scattering amplitude following the general physics principles of Lorentz and gauge invariance and is non–perturbative in nature. The only questionable assumption in its derivation is the use of an unsubtracted dispersion relation. For the proton ($\kappa_p = +1.79$) the GDH sum rule prediction is $-204\,\mu$b, for the neutron ($\kappa_n = -1.91$) it is $-233\,\mu$b. The prediction for the deuteron ($\kappa_d = -0.143$) is $-0.65\,\mu$b. It should be noted that for nuclear targets the lowest–lying inelastic channel is the break–up reaction, in contrast to photoabsorption on the nucleon where the lowest–lying inelastic channel corresponds to single pion production.

No test of the GDH sum rule was hitherto performed due to the lack of polarised targets and suitable real–photon beams. Only recently, first results of an experiment on polarised protons in a limited beam energy range have been published [4]. Using extrapolations into the unmeasured regions, (1) for the proton seems to be satisfied within the experimental uncertainties. Further real–photon experiments are underway at various laboratories to extend the energy range of the measurements [5,6].

The GDH integral can be generalised to non–zero photon virtuality Q^2 in terms of the helicity–dependent virtual–photon absorption cross sections $\sigma^{\rightrightarrows}$ and $\sigma^{\rightleftarrows}$ [7,8]:

$$I_{GDH}(Q^2) = \int_{\nu_0}^{\infty} \left[\sigma^{\rightrightarrows}(\nu, Q^2) - \sigma^{\rightleftarrows}(\nu, Q^2)\right] \frac{d\nu}{\nu}. \qquad (2)$$

The cross section difference appearing in the integrand is given by

$$\Delta\sigma = \sigma^{\rightrightarrows} - \sigma^{\rightleftarrows} = \frac{8\pi^2\alpha}{M_t K}\tilde{A}_1 F_1. \qquad (3)$$

In terms of photon–nucleon (nucleus) helicity states this relation is valid for any target; in case of the deuteron it comprises a mixture of vector and tensor states. Here $\tilde{A}_1$ is the photon–nucleon (nucleus) helicity asymmetry, F_1 the unpolarised nucleon (nucleus) structure function and K the virtual–photon flux factor.

Various generalisations of the GDH integral have been considered in the literature. The difference lies in the choice made for K. In the notation of [8] three such generalisations were considered. In terms of $\tilde{A}_1$ and F_1 they read:

$$I_A(Q^2) = \frac{8\pi^2\alpha}{Q^2}\int_0^{x_0} \tilde{A}_1 F_1 dx, \tag{4}$$

$$I_B(Q^2) = \frac{8\pi^2\alpha}{Q^2}\int_0^{x_0} \frac{1}{\sqrt{1+\gamma^2}}\tilde{A}_1 F_1 dx, \tag{5}$$

$$I_C(Q^2) = \frac{8\pi^2\alpha}{Q^2}\int_0^{x_0} \frac{1}{1-x}\tilde{A}_1 F_1 dx, \tag{6}$$

with $x = Q^2/2M\nu$. I_A corresponds to the case $K = \nu$. The Gilman notation $K = \nu\sqrt{1+\gamma^2}$ [17] has been used for I_B while for I_C the Hand convention $K = \nu(1-x)$ [18] was chosen. They all are numerically close to each other in the limits of deep inelastic scattering and real–photon absorption, but lead to different numerical results for intermediate Q^2. As was pointed out in [8], the generalisation given in (5) is most clearly related to photoabsorption cross sections. Hence, the generalisation used for the figures in this paper is I_B. The full numerical results will be given for all three prescriptions.

When considering a nucleon target (spin $\frac{1}{2}$, mass M) the photon helicity asymmetry $\tilde{A}_1$ is identical to the longitudinal virtual–photon asymmetry A_1 and the generalised GDH integral can be written in terms of the spin structure functions g_1 and g_2 as:

$$I_{GDH}(Q^2) = \frac{8\pi^2\alpha}{M}\int_0^{x_0} \frac{g_1(x,Q^2) - \gamma^2 g_2(x,Q^2)}{K}\frac{dx}{x}, \tag{7}$$

where g_1 and g_2 are the polarised structure functions of the nucleon, $\gamma^2 = Q^2/\nu^2$, $x_0 = Q^2/2M\nu_0$.

Examining the generalised GDH integral provides a way to study the transition from polarised real–photon absorption ($Q^2 = 0$) on the nucleon to polarised deep inelastic lepton scattering (DIS). In other words, it constitutes an observable that allows the study of the transition from the non–perturbative regime at low Q^2 to the perturbative regime at high Q^2. Since the generalised GDH integral is calculated for inelastic reactions, elastic scattering is excluded from its calculation. As has been pointed out in [9], the elastic contribution to the photon cross section becomes the dominant one below $Q^2 \simeq 0.5$ GeV^2; it has to be taken into account when comparing with twist expansions of the first moment of the spin structure function g_1. In the kinematic region considered in this paper, elastic contributions are expected to be small.

Assuming that the Burkhardt – Cottingham sum rule

$$\int_0^1 g_2(x,Q^2)dx = 0 \tag{8}$$

holds in good approximation due to the relatively large Q^2 values considered in this paper, then (7) simplifies to

$$I_A(Q^2) = \frac{16\pi^2\alpha}{Q^2}\Gamma_1(Q^2). \tag{9}$$

As Q^2 becomes larger, the other generalisations I_B and eventually I_C also converge to this value. The first moment of the spin structure function g_1, $\Gamma_1 = \int_0^1 g_1(x)dx$, is predicted to have at large Q^2 only a logarithmic Q^2 dependence from QCD evolution. Since for the proton $\Gamma_1^p > 0$ for higher Q^2, I^p_{GDH} must change sign as Q^2 approaches zero in order to reach the negative value predicted by the GDH sum rule at the real–photon point. The different generalisations lead to different values for the expected zero crossing needed to connect the negative value predicted by (1) with the positive value required by measurements of Γ_1^p in the DIS limit. For the neutron Γ_1^n is negative for all measured Q^2.

The difference of the GDH integral for the proton and the neutron, $I^p_{GDH} - I^n_{GDH}$, is of great interest. In the real–photon case, the GDH sum rule gives $I^p_{GDH} - I^n_{GDH} = 29\mu$b, with a sign opposite to what results from multipole analyses of meson photoproduction data [10]. In the Bjorken limit the difference $\Gamma_1^p - \Gamma_1^n$ is given by the Bjorken sum rule. It can be derived using only current algebra and isospin symmetry [11]. This sum rule relates the difference of the first moments of g_1^p and g_1^n at fixed Q^2 to the well–measured neutron beta–decay coupling constant $g_a = |g_A/g_V| = 1.2670 \pm 0.0035$ [12]:

$$\Gamma_1^p - \Gamma_1^n = \frac{1}{6}\cdot g_a \cdot C_{ns}(\alpha_s(Q^2)), \tag{10}$$

where C_{ns} is the non–singlet QCD correction calculated thus far up to $\mathcal{O}(\alpha_s^3)$ in the modified minimal subtraction ($\overline{MS}$) scheme [13]. Experimental verification of the Bjorken sum rule at finite Q^2 provides a fundamental test of QCD. A measurement of $I^p_{GDH} - I^n_{GDH}$ at large enough Q^2 provides such a test. Previous measurements are consistent with the sum rule when perturbative QCD corrections are included [14–16].

The Q^2–dependence of the generalised GDH integral can be studied separately in the DIS region, characterised by large photon–nucleon invariant mass squared $W^2 = M^2 + 2M\nu - Q^2$, and in the nucleon–resonance region where W^2 amounts to only a few GeV^2. Several experiments measure the generalised GDH integral at low and intermediate Q^2, but cover kinematically only the low–W^2 region [19–21]. On the other hand, the high–W^2 contribution to the generalised GDH integral is found to be sizeable and essential to any estimate of the total integral [22,23]. Preliminary data from real–photon experiments at higher energies support this statement [5]. The kinematics of the HERMES experiment allow the study of the Q^2–development of the generalised GDH integral simultaneously in both the nucleon-resonance and DIS regions.

In Sect. 2 the experimental setup for data taken with a deuteron (proton) target will be described followed by a description of the analysis procedure for both targets in

Sect. 3. The results for the deuteron nucleus are presented in Sect. 4 together with the proton data re–analysed with respect to [23] using an updated value for the target polarisation. From these two data sets the value of I^n_{GDH} is calculated in Sect. 5. Here the assumption is made that in the kinematical range under consideration, nuclear effects are small and the deuteron can be treated as consisting of two quasi–free nucleons. The results on the deuteron nucleus, the proton and the neutron are discussed in Sect. 6. From the values on the proton and neutron, the proton–neutron difference is calculated and compared to the Bjorken sum rule prediction in Sect. 7. A summary of the paper is given in Sect. 8.

2 Experiment

HERMES data on the deuteron target were taken in 1998 to 2000 with a 27.57 GeV beam of longitudinally polarised positrons incident on a longitudinally polarised atomic Deuterium gas target internal to the HERA storage ring at DESY. Data on the proton were taken in 1997 using a longitudinally polarised atomic Hydrogen target. The lepton beam polarisation was measured continously using Compton backscattering of circularly polarised laser light [24,25]. The average beam polarisation for the deuteron (proton) data set was 0.55 (0.55) with a fractional systematic uncertainty of 2.0% (3.4%).

The HERMES polarised gas target [26] consists of polarised atomic D (H) confined in a storage cell. It is fed with nuclear–polarised atoms by an atomic–beam source based on Stern–Gerlach separation [27] and provides an areal target density of about 2×10^{14} (7×10^{13}) atoms/cm^2. The nuclear polarisation of atoms and the atomic fraction are continously measured with a Breit–Rabi polarimeter [28] and a target gas analyser [29], respectively. The polarisation of the atoms can be flipped within short time intervals providing both vector–polarisation states and thus minimising systematic effects in spin–asymmetry measurements. The average value of the target polarisation for the deuteron (proton) data was 0.85 (0.85) with a fractional systematic uncertainty of 3.5 (3.8)%. The value of the proton target polarisation used for the data presented in this paper has been updated with respect to [23] making use of improved knowledge of sampling corrections and treatment of molecular polarisation [30]. The luminosity was monitored by detecting Bhabha events using calorimeter detectors close to the beam pipe [31]. The integrated luminosity per nucleon of the deuteron (proton) data set was 222 pb^{-1} (70 pb^{-1}).

Scattered positrons, as well as coincident hadrons, were detected by the HERMES spectrometer [32]. Positrons were distinguished from hadrons with an average efficiency of 99% and a hadron contamination of less than 1% using the information from an electromagnetic calorimeter, a transition–radiation detector, a preshower scintillation counter and a Cherenkov counter. Only the information on the scattered positron was used in this analysis.

3 Data analysis

In the following, the analysis procedure used for the deuteron data is given. The analysis procedure and treatment of systematic uncertainties have been taken from [22,33] and are detailed in [23], where the same analysis for the proton data was performed. For completeness, the values and parametrisations used in the latter are given below. Note that, compared to [22], the proton data set has been re–analysed in the full kinematic range of [23] to optimise the binning of the kinematically more restricted nucleon-resonance region, where the detector acceptance prevents the full coverage over Q^2.

The kinematic requirements imposed on the scattered positrons in the analysis were identical for both targets. The full range in W^2 ($1.0 < W^2 < 45$ GeV^2) was separated into nucleon resonance region ($1.0 < W^2 < 4.2$ GeV^2) and DIS region ($4.2 < W^2 < 45.0$ GeV^2). The Q^2-range $1.2 < Q^2 < 12.0$ GeV^2 was divided into six bins; the same binning as in the proton case was chosen for the analysis of the deuteron data and for the subsequent determination of I^n_{GDH}. After applying data quality criteria, 0.55 (0.13) million events on the deuteron (proton) in the nucleon-resonance region and 8.3 (1.4) million events in the DIS region were selected.

For all positrons detected, the angular resolution was better than 0.6 mrad, the momentum resolution (aside from Bremsstrahlung tails) better than 1.6% and the Q^2–resolution better than 2.2%. The threshold Cherenkov detector used in the proton measurement was replaced by a Ring–imaging Cherenkov detector [34] for the data taking on the deuteron. The additional amount of material led to a slightly worse W^2–resolution of $\delta W^2 \approx 1.0$ GeV^2 for the deuteron as compared to the proton measurement ($\delta W^2 \approx 0.82$ GeV^2). Although these W^2–resolutions do not allow distinguishing individual nucleon resonances, the integral measurement in the nucleon-resonance region is not degraded.

The generalised GDH integral (2) can be re–written for any target in terms of the photon–target helicity asymmetry $\tilde{A}_1$ and the unpolarised structure function F_1:

$$I_{GDH}(Q^2) = \frac{8\pi^2\alpha}{M_t}\int_0^{x_0}\frac{\tilde{A}_1(x,Q^2)F_1(x,Q^2)}{K}\frac{dx}{x}, \quad (11)$$

where K is the virtual–photon flux factor.

The cross–section asymmetry $\tilde{A}_1$ for the absorption of virtual photons was calculated from the measured cross section asymmetry $A_\parallel$ as

$$\tilde{A}_1 = \frac{A_\parallel}{D} - \eta\tilde{A}_2. \quad (12)$$

For spin–$\frac{1}{2}$ targets the photon helicity asymmetry $\tilde{A}_1$ is identical to the longitudinal virtual photon asymmetry A_1 and $\tilde{A}_2$ is identical to A_2. The difference between these two asymmetries is relevant for the deuteron target only. Even here it is considered to be small in the kinematic region examined in this paper and hence will be neglected in the following.

The measured cross section asymmetry $A_\parallel$ is given by

$$A_\parallel = \frac{N^{\overrightarrow{\Leftarrow}} L^{\overrightarrow{\Rightarrow}} - N^{\overrightarrow{\Rightarrow}} L^{\overrightarrow{\Leftarrow}}}{N^{\overrightarrow{\Leftarrow}} L_P^{\overrightarrow{\Rightarrow}} + N^{\overrightarrow{\Rightarrow}} L_P^{\overrightarrow{\Leftarrow}}}. \quad (13)$$

Here N is the number of detected scattered positrons, L is the integrated luminosity corrected for dead time and L_P is the integrated luminosity corrected for dead time and weighted by the product of the beam and target polarisations. The superscript $\overrightarrow{\Rightarrow}(\overrightarrow{\Leftarrow})$ refers to the orientation of the target spin parallel (anti–parallel) to the positron beam polarisation. The kinematic factor η is given by

$$\eta = \frac{\gamma(1 - y - \gamma^2 y^2/4)}{(1 - y/2)(1 + \gamma^2 y/2)}, \quad (14)$$

where $y = \nu/E_{beam}$ is the inelasticity of the reaction. The effective polarisation of the photon D

$$D = \frac{y(2-y)(1+\gamma^2 y/2)}{y^2(1+\gamma^2)(1-2m_e^2/Q^2) + 2(1-y-\gamma^2 y^2/4)(1+R)} \quad (15)$$

depends also on $R = \sigma_L/\sigma_T$, the ratio of the absorption cross sections for longitudinal and transverse virtual photons and the electron mass m_e. A_2 is related to longitudinal–transverse photon–nucleon interference and is not measured in the present experiment. In the DIS region A_2 can be parametrised in a general form as $A_2 = cMx/\sqrt{Q^2}$, where c is a constant determined from a fit to the data given in [14,15] as $c = 0.20$ (0.53) for the deuteron (proton). In the nucleon-resonance region no data are available for the deuteron and $A_2 = 0$ was chosen, while for the proton a constant value of $A_2 = 0.06 \pm 0.16$ was adopted as obtained from SLAC measurements at $Q^2 = 3\text{GeV}^2$ [14].

Radiative effects for both targets were calculated using the codes described in [35]. They were found not to exceed 7% (4%) of the asymmetry A_1 for the deuteron (proton). On the integral level they do not exceed 2% and were included in the systematic uncertainty.

The fraction of events smeared from the DIS to the nucleon-resonance region and vice versa is evaluated by a Monte Carlo simulation of both regions including radiative and detector effects. Smearing effects in the deep inelastic region have been evaluated for all targets following the procedures described in [23]. The events on the deuteron (proton) were simulated using the parametrisation of F_2 from [36] ([37]) for the DIS region, the elastic form factors from [38]([39]) and the parametrisation of F_2 in the nucleon-resonance region from [40] for both targets. Figure 1 shows the distribution of experimental data as a function of W^2 in comparison with the simulated events on the deuteron. It is apparent that the shape of the simulated distribution agrees well with the data. Similar agreement has been found for the proton.

For the deuteron (proton) case, the relative contaminations from the quasi–elastic (elastic) and deep inelastic region in the nucleon-resonance region range from 15% (10%) to 3% (2%) and from 11% (7%) to 23% (16%) respectively, as Q^2 increases from 1.2 GeV^2 to 12.0 GeV^2.

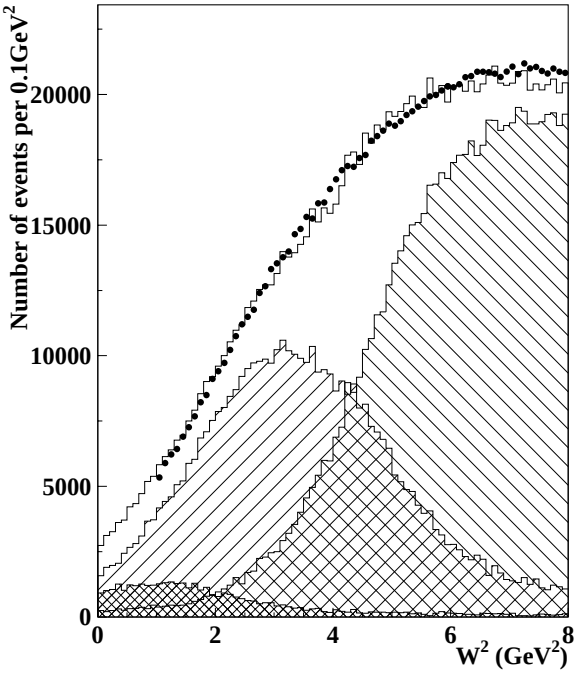

Fig. 1. Comparison of deuteron data with Monte Carlo simulations for the nucleon-resonance region as a function of W^2. The total simulated distribution has been normalised to the data. The cross–hatched area represents the contribution from quasi–elastic scattering, while the lined areas show the contribution from the nucleon-resonance region (left) and from the DIS region (right). The solid line indicates the sum of all simulated events and compares favourably with the data points. The statistical uncertainties of the data are covered by the symbols

The fraction of events smeared from the nucleon-resonance region to the deep inelastic region ranged from 2.9% (2.5%) to 0.5% (0.2%), respectively. Smearing from the elastic region to the DIS region can be neglected in the present experiment.

To evaluate the systematic uncertainty from smearing, two different assumptions on A_1 for the deuteron (proton) have been used: a polynomial representation $A_1 = -0.0307 + 0.92x - 0.28x^2$ (power law $A_1 = x^{0.727}$) that smoothly extends the DIS behaviour for the asymmetry into the nucleon-resonance region [41]; and for both targets a step function ($A_1 = -0.5$ for $W^2 < 1.8$ GeV^2 and $A_1 = +1.0$ for 1.8 GeV^2 $< W^2 <$ 4.2 GeV^2) that is suggested by the hypothesis of the possible dominance of the P_{33}–resonance at low W^2 and of the S_{11}–resonance at higher W^2 (see e.g. [42]). The combined systematic uncertainty in the partial integrals from smearing and radiative effects does not exceed 14% (10%) for the deuteron (proton) data. In both cases, smearing gives by far the dominant contribution.

4 Results for deuteron and proton

The GDH integrals for the deuteron and proton were evaluated following the procedure described in the previous

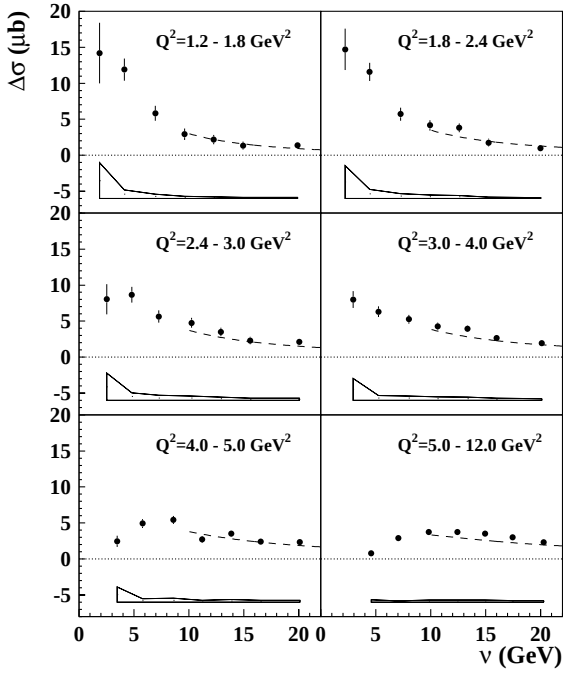

Fig. 2. The cross section difference $\Delta\sigma$ obtained for the deuteron nucleus as a function of the virtual photon energy ν for various bins in Q^2. The dashed curves represent the parametrisation used to extrapolate into the unmeasured region at high W^2

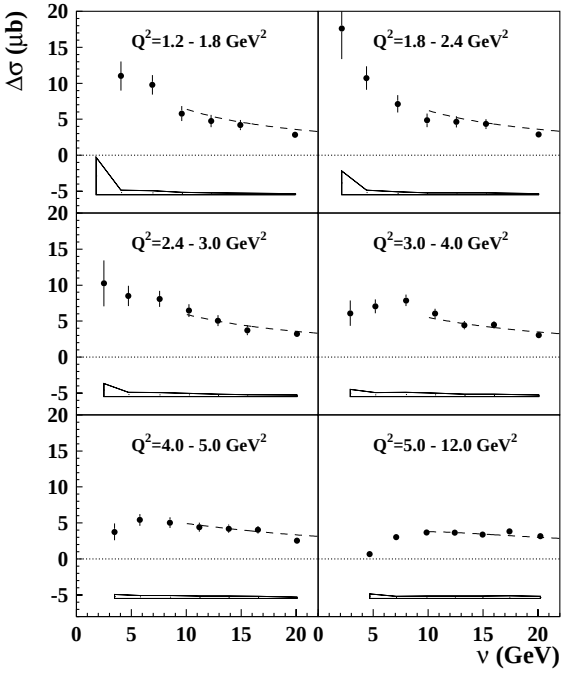

Fig. 3. The cross section difference $\Delta\sigma$ obtained for the proton target as a function of the virtual photon energy ν for various bins in Q^2. Note that for the upper left plot the first data point corresponding to 28.18 ± 6.79 μb at $\nu = 1.8$ GeV is off scale. The dashed curves represent the parametrisation used to extrapolate into the unmeasured region at high W^2

section. The nucleon–resonance region and the DIS region were treated separately. The large W^2–range covered by the HERMES experiment allows essentially the first experimental determination of the complete generalised GDH integral for the deuteron, proton and neutron.

The GDH integral I^d_{GDH} for the deuteron was evaluated using (11) in both the nucleon-resonance region and the DIS region. Here and in the following I^d_{GDH} is understood as the generalised GDH integral for the deuteron *nucleus*. The unpolarised structure function $F_1^d = F_2^d(1+\gamma^2)/(2x(1+R^d))$ was calculated in the nucleon–resonance region from a modification of the parametrisation of F_2^d given in [40] that accounts for nucleon resonance excitation assuming $R^d = \sigma_L/\sigma_T$ to be constant and equal to 0.18 in the whole W^2–range. In the DIS region F_1^d for the deuteron was calculated following a parametrisation of F_2^d from [36]. In the same kinematic region R was chosen according to a fit in [43]. Note that due to cancellations between the R^d dependences of F_1^d and D at low y the final result is affected by at most 2% by a particular choice of R^d. The W^2–dependence of the integrand F_1^d/K in the individual bins was fully accounted for in the integration.

The integrand $\Delta\sigma$ used to calculate I^d_{GDH} for the deuteron target is shown in Fig. 2 as a function of ν for the various bins in Q^2. For the proton case the corresponding values for $\Delta\sigma$ are shown in Fig. 3. In both cases, the extrapolation into the unmeasured region for $W^2 > 45$ GeV^2 was done using a multiple–Reggeon exchange parametrisation [44] for $\Delta\sigma$ at high energy. The resulting contributions are given in Table 1 and range for the deuteron from -0.07 μb at $Q^2 = 1.5$ GeV^2 to 1.53 μb at $Q^2 = 6.5$ GeV^2. The corresponding contributions for the proton amount to about 3.5 μb for all Q^2–bins.

The generalised GDH integrals for the deuteron data, calculated in the nucleon-resonance region, in the DIS region and over the full W^2–range, are depicted in Fig. 4. The statistical and systematic uncertainties of the full I_{GDH} are clearly dominated by the uncertainties in the nucleon-resonance region. They are particularly large due to the smallness of D and the large size of η accentuating the uncertainties in A_2^d, which amounts to 30% of the nucleon-resonance contribution. The systematic uncertainty on A_2^d in the DIS region does not contribute significantly. The systematic uncertainty for the extrapolation to the unmeasured region at high W^2 of 5% has been taken into account. Further sources of systematic uncertainties include the beam and target polarisations (5.5%), the spectrometer geometry (2.5%), the combined smearing and radiative effects (14% of the partial integrals) and the knowledge of F_2 (5%). The total systematic uncertainty of the total GDH integral ranges from 16% at $Q^2 = 1.5$ GeV^2 to 7.5% at $Q^2 = 6.5$ GeV^2. For the systematic uncertainties of the nucleon-resonance and DIS regions, independent sources of systematic uncertainties were added in quadrature, while the systematic uncertainties stemming from smearing effects and the knowledge of F_2^d were added linearly. Only smearing effects from the quasi–elastic region to the measured range of W^2 had to be taken into account for the total integral, thus reduc-

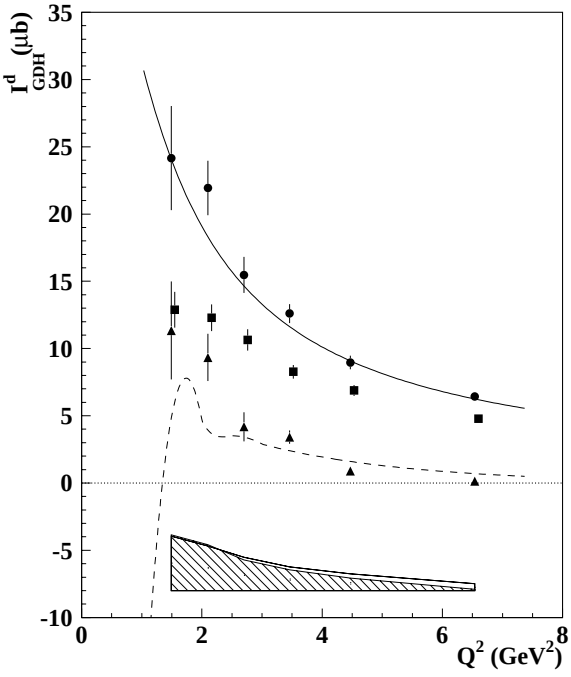

Fig. 4. The generalised GDH integral I^d_{GDH} for the deuteron nucleus, shown as a function of Q^2 for the three kinematic regions considered: nucleon-resonance region (triangles), DIS region (squares), and full W^2–region (circles) including extrapolation to the unmeasured part. The error bars show the statistical uncertainties. The solid curve is taken from [46] and represents a prediction for the full I^d_{GDH}. The dashed curve represents a model for the nucleon-resonance region from [45]. The systematic uncertainties of the full integral are given as a band; the hatched area inside represents the systematic uncertainty of the nucleon-resonance region alone. Note that some data points are slightly shifted for better visibility

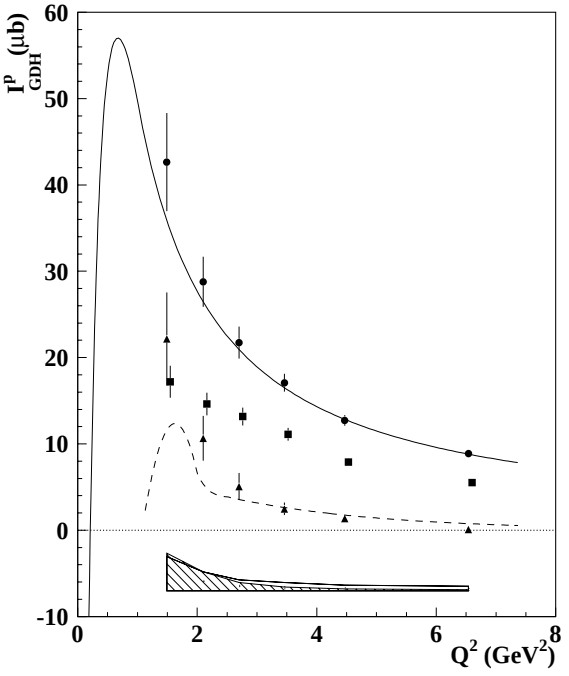

Fig. 5. The generalised GDH integral I^p_{GDH} for the proton using the same notation as in Fig. 4. The solid curve is taken from [46], the dashed curve follows the model of [45]. The data were published earlier in [23], but are re–analysed for the present paper using improved knowledge on the target polarisation. The band representing the systematic uncertainties is given for the convention defined in Fig. 4

ing considerably its systematic uncertainty due to smearing compared to the integrals calculated separately in the nucleon-resonance and DIS regions.

The generalised GDH integrals for the proton data reanalysed using an updated value of the target polarisation, calculated in the nucleon-resonance region, in the DIS region and over the full W^2–range, are depicted in Fig. 5. For both targets, the contribution of the nucleon-resonance region decreases faster than that of the DIS region as a function of Q^2. The latter dominates I^d_{GDH} and I^p_{GDH} for $Q^2 > 3.0$ GeV^2 and remains sizeable even at the lowest measured Q^2. The nucleon-resonance contribution shown in Fig. 4 and Fig. 5 respectively for the deuteron and proton is compared to a curve representing the prediction of the model of [45]. This model is based on a helicity–dependent sum over the first, second and third nucleon–resonance regions using experimental resonance parameters, but assuming infinitely narrow resonances. The threshold region was taken into account in the first nucleon–resonance region. Within the total experimental uncertainties this model describes the data.

The data for the full integral on both the deuteron and the proton target are compared to a model based on the leading twist Q^2–evolution of the first moments of the two polarised structure functions g_1 and g_2 without consideration of any explicit nucleon–resonance contribution [46,47]. In this model, the low–Q^2 behaviour of g_2 is governed by the Q^2–dependence of a linear combination of the electric and magnetic Sachs form factors. The model predicts the shape. It predictions thus depend on the experimental value for Γ_1 at asymptotically large Q^2 and on the Q^2–dependence of the Sachs form factors at low Q^2. The normalisations for asymptotically large Q^2 was taken from the present data. They were evaluated from the Q^2–dependencies of $I^{p,n}_{GDH}$ with the $1/Q^2$–dependence expected from leading twist devided out. Fitted by straight lines the results are $\Gamma_1^p = 0.129 \pm 0.006$ and $\Gamma_1^n = -0.030 \pm 0.007$ (cf. Figure 9). The parameterisation of the form factors was taken from [46]. The model describes the data on the proton very well. No explicit prediction for the deuteron is given; thus the deuteron is modelled as the sum of proton and neutron. Nevertheless, the model prediction also agrees well the deuteron data.

5 Neutron results from deuteron and proton

The extraction of the generalised GDH integral for the neutron from data taken on the deuteron and the proton requires nuclear effects such as Fermi motion and the depolarising effect of the D–state to be taken into account.

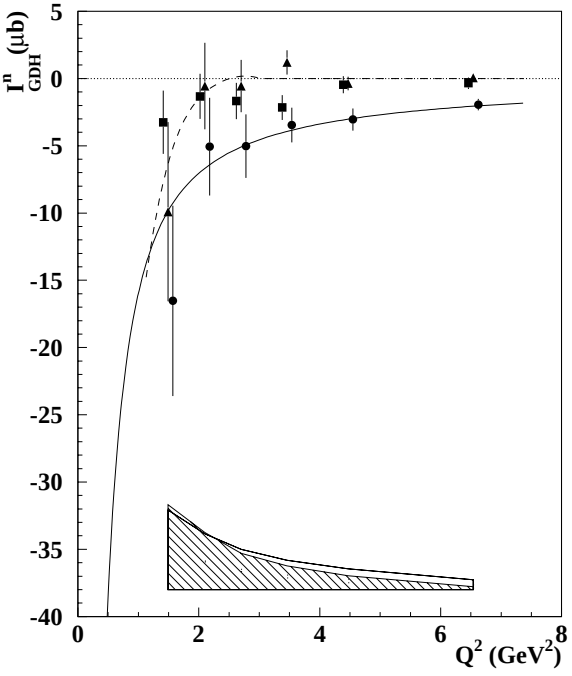

Fig. 6. The generalised GDH integral I^n_{GDH} for the neutron obtained from the deuteron and proton using the same notation as in Fig. 4 for the symbols and theoretical curves

These questions were addressed in [48]. Following their model, the integral I^n_{GDH} for the neutron was calculated from the results I^d_{GDH} on the deuteron, as obtained in this analysis, and those on the proton I^p_{GDH} re–analysed following the procedure detailed in [23]:

$$I^n_{GDH} = \frac{I^d_{GDH}}{1 - 1.5\omega_d} - I^p_{GDH}. \qquad (16)$$

Here $\omega_d = 0.050 \pm 0.010$ [49] is the probability of the deuteron to be in a D–state. It has been shown in [48] that although the uncertainties in the structure functions in the integrand of (11) may be large, the resulting contribution to the systematic uncertainty for the integral I^n_{GDH} due to nuclear effects does not exceed 3%. This combined with the uncertainty in ω_d leads to an additional systematic uncertainty on I^n_{GDH} of 4%. No further assumptions, in particular not on F^n_2, A^n_2 and R, are needed to derive the generalised GDH integral for the neutron using (16).

In the real–photon case, the application of (16) is not straightforward, since significant contributions from photodisintegration and coherent photoproduction must be taken into account [50]. For virtual photons three different regions can be distinguished. For $Q^2 > 1\text{GeV}^2$ the generalised GDH integral can be described by the spin structure functions g_1 and g_2 taking twist–2 and twist–3 contributions into account (cf. (7)). Higher twist contributions are suppressed by powers of $1/Q^2$; (16) holds. For $Q^2_0 < Q^2 < 1$ GeV^2, (16) holds, but the GDH–integrals for proton and neutron deviate substantially from the g_1 and g_2 (twist–2 and twist–3) contributions. In this region, the Operator Product Expansion has already broken down and one has to resort to model assumptions like those of [46,47]. The relevant scale Q^2_0 was estimated in [51] to be $Q^2_0 \sim m^2_\pi$. Finally, for $Q^2 < Q^2_0$ (16) is no longer valid.

In Fig. 6 the results for I^n_{GDH} obtained from the deuteron and proton data in three W^2–regions are shown together with model predictions following [45] and [46]. As in the proton case, the contribution from the nucleon resonance region decreases faster with increasing Q^2 compared to the contribution from the DIS region. The data are well described by the resonance model. The contribution from the extrapolation to high W^2 is dominant for $Q^2 > 2.0$ GeV^2 and remains sizeable down to the lowest measured Q^2 (cf. Table 1). In agreement with measurements of the neutron spin structure function g^n_1 and as expected from recent measurements of polarised quark distributions [52], I^n_{GDH} is negative and of smaller absolute size than the proton value. Within the total experimental uncertainties, the model prediction of [46] agrees well with the neutron data for the full integral.

Results on I^n_{GDH} were also obtained from a previous measurement on a ^{3}He target [22]. The neutron asymmetry was obtained from the ^{3}He asymmetry taking into account nuclear effects, the relative polarisation of the neutron and two protons, as well as a fit to the data for A^p_1. Note that the lower W^2–limit for the data taken on ^{3}He was 4 GeV^2 and thus slightly different from the cut at 4.2 GeV^2 used in the deuteron analysis. Both data sets are shown in Fig. 7 and agree within their respective uncertainties.

6 Discussion of results

In Table 2 the final results are presented for the full generalised GDH integrals on the deuteron, the proton and the neutron in bins of Q^2 and for the three generalisations (4, 5, 6) considered in the literature. Significant differences between the integral values in various generalisations are observed. While I_A and I_B remain comparable at the measured Q^2 values due to the smallness of γ^2, the $\frac{1}{1-x}$ weighting introduced by the Hand notation in I_C leads to sizeable differences. The results will be discussed referring to the generalisation I_B.

As mentioned above, the final results for the proton and for the neutron, as presented in Fig. 5 and Fig. 6, show that the contribution of the nucleon resonance region to the full generalised GDH integral is small for $Q^2 > 3$ GeV^2 and the contribution from the DIS region remains sizeable down to the lowest measured Q^2 values. Numerical values following the generalisation I_B are given in Table 1.

The results for the full generalised GDH integrals on the deuteron, proton and neutron are shown together in Fig. 8. As noted above, they agree well within the total uncertainties with a prediction of [46] based on the leading twist Q^2–evolution of the two polarised structure functions g_1 and g_2 without consideration of any explicit nucleon–resonance contribution. Although in the neutron case the poorer knowledge of input data for this model leads to a larger uncertainty, a similar description of the data compared to the proton case is achieved. No turn–over is observed in the measured range that would be re-

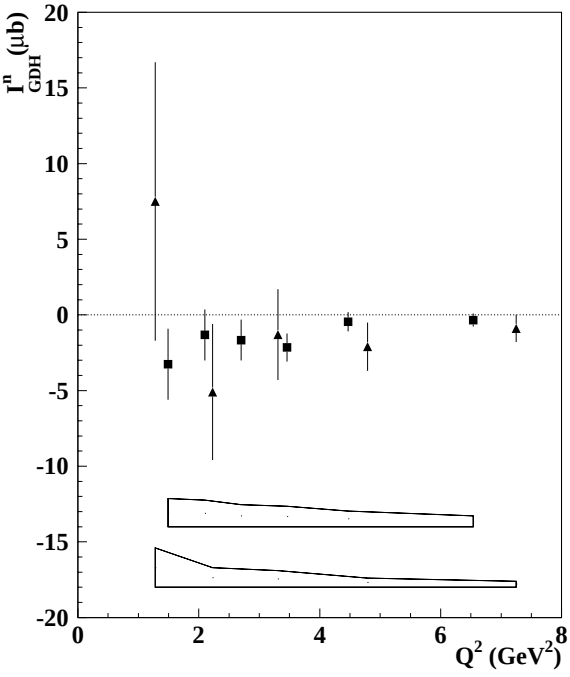

Fig. 7. The generalised GDH integral I^n_{GDH} in the DIS region for the neutron (squares) obtained combining deuteron and proton data, shown in comparison to the results obtained on ^{3}He (triangles) [22]. The lower W^2–limit for the latter was $W^2 > 4.0$ GeV^2 while for the former $W^2 > 4.2$ GeV^2 was used. The error bars represent the statistical uncertainties. The systematic uncertainties for each data set are given as error bands (deuteron top, ^{3}He bottom)

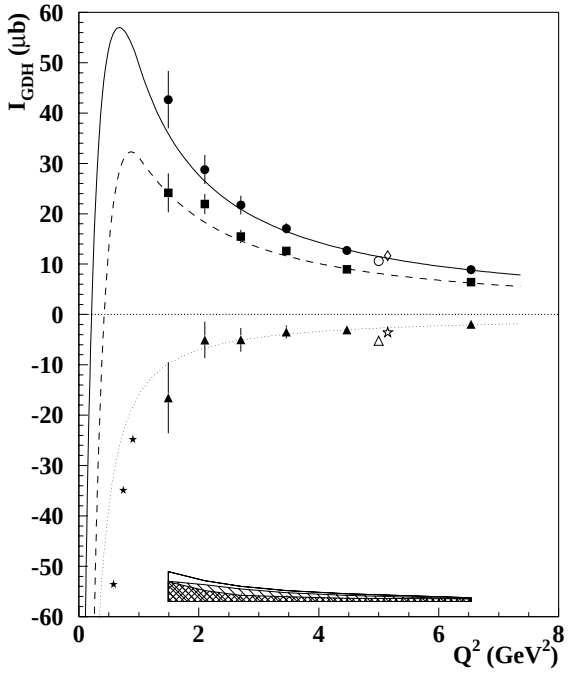

Fig. 8. The Q^2–dependence of the generalised GDH integrals, calculated over the full W^2–region, for the deuteron nucleus (squares), proton (circles) and neutron (triangles). The latter was obtained from the deuteron and proton data. The curves shown are the predictions for the various targets according to [46]. The error bars represent the statistical uncertainties. The bands represent the systematic uncertainties (open: neutron, lined: deuteron, cross–hatched: proton). The open symbols at $Q^2 = 5$ GeV^2 represent the measurements from [14] (shifted to the left) and [15] (shifted to the right) on proton and neutron. The stars represent the three highest Q^2 bins of the neutron measurement from [21] including an extrapolation for the unmeasured DIS region

quired for the generalised GDH integral on the proton or the deuteron to meet the GDH sum rule predictions at $Q^2 = 0$. Preliminary data from [19,20] and a recent theoretical evaluation indicate that this sign change happens at a value of Q^2 much lower than the range considered in this analysis [53].

At large Q^2 the generalised GDH integral is connected to the first moment of the spin structure function g_1 (9). For $Q^2 > 3$ GeV^2 the generalised GDH integral is completely dominated by the DIS region. The data presented in this paper agree with the most recent values for the first moments of the spin structure functions measured on the proton by E–155 (E–143) $\Gamma_1^p = 0.118 \pm 0.004 \pm 0.007$ $(\Gamma_1^p = 0.129 \pm 0.003 \pm 0.010)$ and on the neutron measured by E–155 (E–143) $\Gamma_1^n = -0.058 \pm 0.005 \pm 0.008$ $(\Gamma_1^n = -0.034 \pm 0.007 \pm 0.016)$ evaluated at $Q^2 = 5\text{GeV}^2$ [14,15]. These values correspond to $I^p_{GDH}(Q^2 = 5\text{GeV}^2) = 10.59 \pm 0.36 \pm 0.73$ $(11.85 \pm 0.28 \pm 0.92)$ μb and $I^n_{GDH}(Q^2 = 5\text{GeV}^2) = -5.21 \pm 0.45 \pm 0.72$ $(-3.12 \pm 0.64 \pm 1.47)$ μb, for the proton and the neutron respectively, and are shown together with the present data in Fig. 8.

The Q^2–behaviour of I_{GDH} for proton and neutron can be more clearly studied when dividing out from I_{GDH} the $1/Q^2$–dependence expected from leading twist. According to (9), I_{GDH} is then expected to show a logarithmic Q^2–dependence, similar to Γ_1. The result is shown in Fig. 9. Any contributions from resonance form factors or higher–twist contributions should become visible as a deviation from a flat line. Considering the statistical and systematic uncertainties of the present measurement, no deviation from a leading–twist behaviour can be seen. In other words, the experimental data obtained for the proton and the neutron are consistent with the naive expectation that the $1/Q^2$ expansion is a good approximation down to $Q^2 \simeq 2\text{GeV}^2$. As discussed in the introduction the elastic part ($x = 1$) has to be included for a complete comparison to a twist expansion of Γ_1. However, this is not a relevant contribution in the kinematic range considered.

7 Combined results for the proton and the neutron

The data obtained for the proton and neutron over a large range in Q^2 and W^2 offer a unique possibility to evaluate the proton–neutron difference of the generalised GDH integral. This difference is shown in Fig. 10. It is expected to be less sensitive to higher twist effects or contributions

Table 1. The generalised GDH integral I_B for the deuteron, proton and neutron given in μb per nucleus for the full W^2–region, the nucleon resonance region and the DIS region and various values of Q^2 in GeV^2. The statistical and systematic uncertainties are given. The last three rows show the integral values for the extrapolation to higher W^2, for the deuteron, proton and neutron. Note that the systematic error on the total integral is reduced compared to the integral in the nucleon-resonance and DIS regions, since smearing between these regions is not to be taken into account

Q^2	1.5	2.1	2.7	3.5	4.5	6.5
$I^d_{\rm tot}$	24.2±3.9 ± 3.9	21.9±2.0 ± 3.2	15.5±1.3 ± 2.4	12.6±0.7 ± 1.7	9.0±0.5 ± 1.2	6.4±0.3 ± 0.5
$I^d_{\rm res}$	11.4±3.6 ± 4.0	9.3±1.8 ± 3.3	4.2±1.1 ± 2.2	3.4±0.5 ± 1.6	0.9±0.3 ± 0.9	0.1±0.1 ± 0.1
$I^d_{\rm DIS}$	12.9±1.3 ± 1.3	12.3±1.0 ± 1.3	10.6±0.8 ± 1.3	8.3±0.5 ± 0.9	6.9±0.4 ± 0.7	4.8±0.3 ± 0.5
$I^p_{\rm tot}$	42.7±5.7 ± 3.8	28.8±2.9 ± 2.1	21.7±1.9 ± 1.2	17.1±1.0 ± 0.9	12.7±0.6 ± 0.6	8.9±0.3 ± 0.5
$I^p_{\rm res}$	22.2±5.4 ± 4.2	10.7±2.6 ± 2.1	5.0±1.5 ± 0.9	2.5±0.7 ± 0.4	1.3±0.4 ± 0.2	0.1±0.1 ± 0.1
$I^p_{\rm DIS}$	17.2±1.9 ± 1.1	14.6±1.3 ± 1.0	13.2±1.0 ± 1.0	11.1±0.7 ± 0.8	7.9±0.5 ± 0.6	5.5±0.3 ± 0.5
$I^n_{\rm tot}$	−16.5±7.1 ± 5.7	−5.1±3.6 ± 4.0	−5.0±2.4 ± 2.9	−3.5±1.3 ± 2.0	−3.0±0.8 ± 1.4	−1.9±0.4 ± 0.7
$I^n_{\rm res}$	−9.8±6.7 ± 6.1	−0.6±3.2 ± 4.0	−0.6±1.9 ± 2.6	1.2±0.9 ± 1.7	−0.3±0.5 ± 1.0	0.1±0.1 ± 0.2
$I^n_{\rm DIS}$	−3.3±2.3 ± 1.8	−1.3±1.7 ± 1.7	−1.6±1.4 ± 1.7	−2.1±0.9 ± 1.3	−0.4±0.6 ± 1.0	−0.2±0.4 ± 0.7
$I^d_{\rm unm}$	−0.1	0.3	0.7	0.9	1.2	1.5
$I^p_{\rm unm}$	3.3	3.5	3.5	3.5	3.5	3.3
$I^n_{\rm unm}$	−3.4	−3.2	−2.8	−2.6	−2.3	−1.8

Table 2. The generalised GDH integral for the deuteron, proton and neutron, calculated for the full W^2–range, given in μb per nucleus for the generalisations given in (4, 5, 6) following [8] and various values of Q^2 in GeV^2. The statistical and systematic uncertainties are given

Q^2	1.5	2.1	2.7	3.5	4.5	6.5
I^d_A	27.4 ±4.7 ± 4.5	24.5 ±2.4 ± 3.5	16.7 ±1.6 ± 2.6	13.5 ±0.8 ± 1.8	9.4 ±0.5 ± 1.2	6.6 ±0.3 ± 0.5
I^d_B	24.2 ±3.9 ± 3.9	21.9 ±2.0 ± 3.2	15.5 ±1.3 ± 2.4	12.6 ±0.7 ± 1.7	9.0 ±0.5 ± 1.2	6.4 ±0.3 ± 0.5
I^d_C	44.9 ±9.3 ± 7.3	43.3 ±5.2 ± 6.3	28.3 ±3.6 ± 4.4	24.5 ±1.9 ± 3.3	14.9 ±1.3 ± 2.0	9.4 ±0.4 ± 0.8
I^p_A	48.7 ±6.9 ± 4.3	31.7 ±3.4 ± 2.3	23.2 ±2.2 ± 1.3	17.9 ±1.1 ± 1.0	13.3 ±0.7 ± 0.6	9.0 ±0.3 ± 0.5
I^p_B	42.7 ±5.7 ± 3.8	28.8 ±2.9 ± 2.1	21.7 ±1.9 ± 1.2	17.1 ±1.0 ± 0.9	12.7 ±0.6 ± 0.6	8.9 ±0.3 ± 0.5
I^p_C	81.7 ±14.0 ± 7.4	53.4 ±7.7 ± 3.9	37.4 ±5.3 ± 2.1	27.8 ±2.8 ± 1.6	20.4 ±1.9 ± 0.9	11.8 ±0.4 ± 0.7
I^n_A	−19.0 ±8.6 ± 6.5	−5.2 ±4.3 ± 4.5	−5.1 ±2.8 ± 3.1	−3.3 ±1.4 ± 2.2	−3.1 ±0.9 ± 1.5	−1.9 ±0.4 ± 0.7
I^n_B	−16.5 ±7.1 ± 5.7	−5.1 ±3.6 ± 4.0	−5.0 ±2.3 ± 2.9	−3.5 ±1.3 ± 2.0	−3.0 ±0.8 ± 1.4	−2.0 ±0.4 ± 0.7
I^n_C	−33.1 ±17.2 ± 10.8	−6.6 ±9.5 ± 7.8	−6.6 ±6.6 ± 5.1	−1.4 ±3.5 ± 3.8	−4.3 ±2.3 ± 2.3	−1.6 ±0.6 ± 1.0

from nucleon resonances. Within the measured Q^2–range no turn–over at low Q^2 required to meet the GDH sum rule prediction of 29 μb for $Q^2 = 0$ is observed. The data fall off as $1/Q^2$ indicating that leading twist dominates as expected. A fit to the data using c/Q^2 where c is a constant is shown together with the data in Fig. 10. For the constant $c/(16\pi^2\alpha) = 0.159\pm0.009$ is found, leading to a value $I^p_{GDH} - I^n_{GDH} = 14.3 \pm 0.9 \pm 1.3$ μb at $Q^2 = 5$GeV^2. This result is in agreement with an experimental determination of the Bjorken sum rule by E–155 (E–143), $\Gamma^p_1 - \Gamma^n_1 = 0.176\pm0.003\pm0.007$ $(0.164\pm0.008\pm0.020)$ [14,15] within the respective experimental uncertainties. At $Q^2 = 5$GeV^2 these values correspond to $I^p_{GDH} - I^n_{GDH} = 15.76 \pm 0.27 \pm 0.63$ μb $(14.95 \pm 0.72 \pm 1.79$ $\mu b)$. Within errors, the value for the proton–neutron difference measured in this analysis is also in agreement with the Bjorken–sum–rule prediction of 0.182 ± 0.005 corresponding to $I^p_{GDH} - I^n_{GDH} = 16.33 \pm 0.45$ μb. The Bjorken sum rule was evaluated using (10) at $Q^2 = 5$GeV^2 including corrections up to third–order in α_s and with $\alpha_s(M_Z) = 0.118$.

8 Summary

The generalised GDH integral has been determined for a deuteron target in the kinematic region $1.2 < Q^2 < 12.0$ GeV^2 and $1 < W^2 < 45$ GeV^2 in this paper. Using an updated value of the target polarisation, a corresponding re–analysis of the HERMES proton data as compared to [23] was performed. In both cases the W^2–range was separated at $W^2 = 4.2$ GeV^2 into a region where the nucleon resonances dominate and into the DIS region. Combining both data sets, the generalised GDH integral for the neutron was calculated in the same kinematic regions.

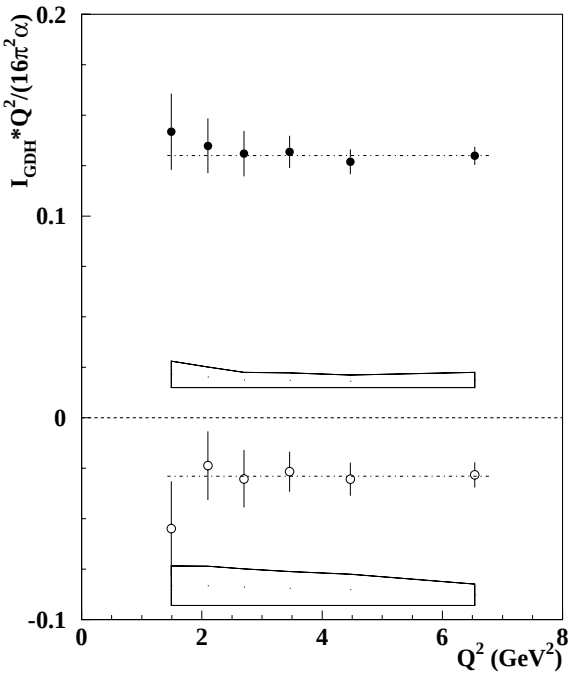

Fig. 9. The Q^2–dependence of the generalised GDH integrals for the proton (filled circles) and neutron(open circles) after the leading–twist dependence, $Q^2/(16\pi^2\alpha)$, has been divided out. The error bars represent the statistical errors. The systematic uncertainties are represented by the respective error bands. The dash–dotted lines are straight line fits to the data

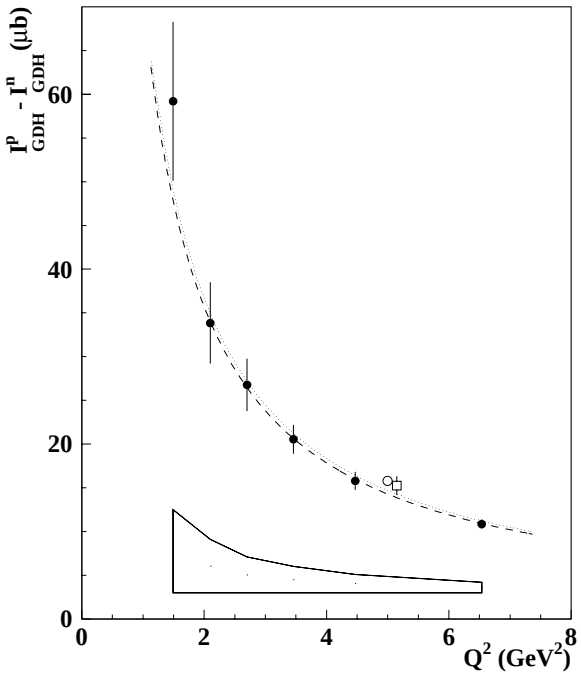

Fig. 10. The Q^2–dependence of the generalised GDH integral for the proton–neutron difference. The dotted curve represent the prediction from [47]. The dashed curve represents a simple $1/Q^2$ fit to the data leading to $I^{p-n}_{GDH}(Q^2 = 5\text{GeV}^2)$ of 14.3 $\pm 0.9 \pm 1.3$ μb. For large Q^2 this difference is expected to obey the Bjorken sum rule. The open symbols represent the measurements of the Bjorken sum rule from [14] (square) and [15] (circle). They are slightly shifted in Q^2 for clearer representation. At $Q^2 = 0$ the GDH sum rule gives a value of 29 μb. The error bars represent the combined statistical uncertainties; the band indicates the systematic uncertainty

These neutron results obtained from the deuteron agree with those obtained earlier on a ^{3}He target in the same kinematic region.

Altogether, a complete set of measurements of the generalised GDH integrals for the deuteron, proton and neutron is available. In all three cases the nucleon-resonance contribution to the generalised integral decreases rapidly with increasing Q^2 and the contribution from the DIS region is still sizeable even at the lowest measured Q^2, emphasising the importance of measuring the GDH integral over a large W^2–range. At larger Q^2 the measured values agree well with measurements of the first moments of the spin structure function g_1.

For the generalised GDH integrals of the proton, the neutron and the proton–neutron difference, the Q^2–dependence is in agreement with a leading–twist behaviour; within the experimental uncertainties it exhibits no significant contribution from either higher twist or resonance form factors. The proton–neutron difference is in agreement with the Bjorken–sum–rule prediction evaluated at $Q^2 = 5\text{GeV}^2$ within the experimental uncertainties.

Acknowledgements. We gratefully acknowledge the DESY management for its support, the staffs at DESY and the collaborating institutions for their significant effort. This work was supported by the FWO–Flanders, Belgium; the Natural Sciences and Engineering Research Council of Canada; the INTAS and RTN network ESOP (contract number 1999-00117) contributions from the European Union; the German Bundesministerium für Bildung und Forschung; the Deutsche Forschungsgemeinschaft (DFG); the Deutscher Akademischer Austauschdienst (DAAD); the Italian Istituto Nazionale di Fisica Nucleare (INFN); Monbusho International Scientific Research Program, JSPS, and Toray Science Foundation of Japan; the Dutch Foundation for Fundamenteel Onderzoek der Materie (FOM); the U. K. Particle Physics and Astronomy Research Council; and the U. S. Department of Energy and National Science Foundation.

References

1. S.B. Gerasimov, Sov. J. Nucl. Phys. **2**, 430 (1966)
2. S.D. Drell, A.C. Hearn, Phys. Rev. Lett. **16**, 908 (1966)
3. G. Altarelli, N. Cabbibo, M. Maiani, Phys. Lett. B **40**, 415 (1972); S. Brodsky, I. Schmidt, Phys. Lett. B **352**, 344 (1995)
4. GDH collaboration, J. Ahrens et al., Phys. Rev. Lett. **87**, 022003 (2001)
5. GDH collaboration, G. Zeitler, πN–Newsletter **16**, 311 (2002)
6. V. Ghazikhanian et al., SLAC–Proposal E–159 (2000); D.Sober et al., CEBAF PR–91–15 (1991)
7. R. Pantförder, PhD Thesis, Universität Bonn (1998), BONN-IR-98-06, hep-ph/9805434 and references therein

8. D. Drechsel, S.S. Kamalov, L. Tiator, Phys. Rev. D **63** (2001), 114010
9. X. Ji, W. Melnitchouk, Phys. Rev. D **56**, R1 (1997)
10. I. Karliner, Phys. Rev. D **7**, 2717 (1973); R.L. Workman, R.A. Arndt, Phys. Rev. D **45**, 1789 (1992); A.M. Sandorfi, C.S. Whisnant, M. Khandaker, Phys. Rev. D **50**, R6681 (1994); D. Drechsel, G. Krein, Phys. Rev. D **58**, 116009 (1998)
11. J.D. Bjorken, Phys. Rev. **148**, 1467 (1966); Phys. Rev. D **1**, 1376 (1970)
12. Particle Data Group, Eur. Phys. J. C **15**, 1 (2000)
13. S. A. Larin, J. A. M. Vermaeseren, Phys. Lett. B **259** (1991) and references therein
14. E–143 Collaboration, K. Abe et al., Phys. Rev. D **58**, 112003 (1998); K. Abe et al., Phys. Rev. Lett. **78**, 815 (1997)
15. E–155 Collaboration, P. L. Anthony et al., Phys. Lett. B **493**, 19 (2000); E–155 Collaboration, P. L. Anthony et al., Phys. Lett. B **463**, 339 (1999)
16. SMC Collaboration, B. Adeva et al., Phys. Rev. D **58**, 112002 (1998)
17. F.J. Gilman, Phys. Rev. **167**, 1365 (1968)
18. L. N. Hand, Phys. Rev. **129**, 1834 (1963)
19. V. Burkert et al., CEBAF PR-91-23, 1991; S. Kuhn et al., CEBAF PR-93-09, 1993; J.P. Chen et al., TJANF PR-97-110, 1997
20. CLAS Collaboration, R. Fatemi et al., Proc. of SPIN 2000: 14th International Spin Physics Symposium, edited by K. Hatanaka et al., Osaka, Japan, AIP Conf. Proc. **570**, 402 (2001)
21. M. Amarian et al., `arXiv:nucl-ex/0205020`, Phys. Rev.Lett. in press; priv. comm
22. HERMES Collaboration, K. Ackerstaff et al., Phys. Lett. B **444**, 531 (1998)
23. HERMES Collaboration, A. Airapetian et al., Phys. Lett. B **494**, 1 (2000)
24. D.P. Barber et al., Phys. Lett. B **343**, 436 (1997)
25. M. Beckmann et al., Nucl. Instr. Meth. A **479**, 334 (2002)
26. J. Stewart, Proc. of the Workshop on Polarised gas targets and polarised beams, edited by R.J. Holt, M.A. Miller, Urbana-Champaign, USA, AIP Conf. Proc. **421**, 69 (1997)
27. F. Stock et al., Nucl. Instr. and Meth. A **343**, 334 (1994)
28. C. Baumgarten et al., Nucl. Instr. and Meth. A **482**, 606 (2002)
29. M. C. Simani, PhD Thesis, Vrije Universtiteit Amsterdam, October 2002
30. HERMES Collaboration, P. Lenisa, talk at the 15th Int. Spin Physics Symposium, Upton/USA, Sept. 2002, to appear in the proceedings
31. Th. Benisch et al., Nucl. Instr. and Meth. A **471**, 314 (2001)
32. HERMES Collaboration, K. Ackerstaff et al., Nucl. Instr. and Meth. A **417**, 230 (1998)
33. HERMES Collaboration, A. Airapetian et al., Phys. Lett. B **442**, 484 (1998)
34. N. Akopov et al., Nucl. Instr. and Meth. A **479**, 511 (2002)
35. I.V. Akushevich, N.M. Shumeiko, J. Phys. G **20**, 513 (1994); I. Akushevich et al., Comput. Phys. Commun. **104**, 201 (1997)
36. NMC Collaboration, M. Arneodo et al., Nucl. Phys. B **371**, 3 (1992)
37. NMC Collaboration, M. Arneodo et al., Phys. Lett. B **364**, 107 (1995)
38. S. Stein et al., Phys. Rev. D **12**, 1884 (1975) and references therein
39. S. I. Bilen'kaya et al., Zh. Eksp. Teor. Fiz. Pis'ma **19**, 613 (1974)
40. A. Bodek, Phys. Rev. D **8**, 2331 (1973)
41. A. P. Nagaitsev et al., JINR Rapid Communications, July 1995, N3(71)-95, 59
42. J. Edelmann, G. Piller, N. Kaiser, W. Weise, Nucl. Phys. A **665**, 125 (2000)
43. L.W. Whitlow et al., Phys. Lett. B **250**, 193 (1990)
44. N. Bianchi, E. Thomas, Phys. Lett. B **450**, 439 (1999)
45. I. G. Aznauryan, Phys. of At. Nucl. **58**, 1014 (1995) and private communication
46. J. Soffer, O.V. Teryaev, Phys. Rev. D **51**, 25 (1995); J. Soffer, O.V. Teryaev, Phys. Rev. Lett. **70**, 3373 (1993)
47. J. Soffer, O.V. Teryaev, Phys.Rev. D **56**, 7458 (1997); J. Soffer, O.V. Teryaev, hep–ph/0207252
48. C. Ciofi degli Atti et al., Phys. Lett. B **376**, 309 (1996)
49. M. Lacombe et al., Phys. Rev. C **21**, 861 (1980); M. J. Zuilhof, J. A. Tjon, Phys. Rev. C **22**, 2369 (1980); A. Yu. Umnikov et al., proceedings of SPIN 1994: 11th Int. Symp. on High Energy Spin Physics, edited by K.J. Heller, S.L. Smith, AIP Conf. Proc. **343** 79
50. H. Arenhövel, G. Kreß, R. Schmidt, P. Wilhelm, Phys. Lett. B **407**, 1 (1997)
51. O.V. Teryaev, talk at XVI International Baldin Seminar "Relativistic Nuclear Physics and Quantum Chromodynamics", Dubna/Russia, June 2002, to appear in the proceedings
52. HERMES Collaboration, K. Ackerstaff et al., Phys. Lett.B **464**, 123 (1999); HERMES Collaboration, M. Beckmann, Proc. of the Workshop on "Testing QCD through Spin Observables on Nuclear Targets", Charlottesville, VA, 2002
53. X. Ji, C.W. Kao, J. Osborne, Phys.Rev. D **61**, 074003 (2000); X. Ji, J. Osborne, J. Phys. G **27**, 127 (2001)